Korean J. Chem. Eng., **27**(3), 791-801 (2010)
DOI: 10.1007/s11814-010-0118-6

Thermogravimetric analysis of longan seed biomass with a two-parallel reactions model

Supunnee Junpirom*, Chaiyot Tangsathitkulchai*,†, and Malee Tangsathitkulchai**

*School of Chemical Engineering, Institute of Engineering, **School of Chemistry, Institute of Science, Suranaree University of Technology, Nakhon Ratchasima 30000, Thailand
(*Received 23 July 2009 • accepted 15 September 2009*)

Abstract−The kinetic analysis of pyrolysis process of longan seed was performed in a thermogravimetric analyzer. All experimental runs were carried out by using an initial sample mass of 15 mg and final temperature of 650 °C under the inert atmosphere of nitrogen. Particle sizes in the range from 0.05-2.1 mm and the heating rates from 5-100 °C/min were employed to investigate their effects on the thermogram and the kinetic parameters. The TG curves generally showed sigmoid shape and displayed one major peak in DTG curve. The main devolatilization of longan seed occurred over the temperature range of 210-330 °C. It was found that heat transfer resistance in a particle could be reduced either by decreasing the size of particle or increasing the heating rate. The thermal decomposition of longan seed could be well described by the two-parallel reactions kinetic model. This analysis of reaction kinetic gave the values of activation energy for the decomposition of the two fractions in the model corresponding closely to those of hemicellulose and lignin.

Key words: Pyrolysis, Devolatilization, Two Parallel Reactions Model, Longan Seed

INTRODUCTION

Biomass can be converted to energy and fuel via four main thermochemical methods: pyrolysis, liquefaction, gasification and combustion [1-4]. Presently, biomass pyrolysis is gaining increasing attention as a potential method to produce solid, liquid or gaseous fuels. In particular, the liquid fuel has many advantages; for example, it can be stored, easily transported, upgraded to high quality fuel or it can be alternatively exploited as a chemical feedstock to recover an array of valuable products [5-9]. The solid product called char can also be used as a raw material to produce a porous carbon adsorbent. Pyrolysis of biomass is a very complex process due to the multiple components of biomass, leading to multitude of reactions that occur simultaneously. It is known that biomass is basically composed of three main fractions of hemicellulose, cellulose and lignin, the compositions of which vary for each type of biomass.

The mechanism of biomass pyrolysis is indeed complicated, involving many thermal reactions with simultaneous heat and mass transfer. There has been considerable research effort to better understand the biomass pyrolysis by proposing simplified models to predict the residual weight, decomposition rate and the kinetic parameters. Normally, in many of the kinetic formulations of thermal decomposition reactions, it has been assumed that isothermal homogeneous gas or liquid phase kinetic equations can be applied [10]. Numerous pyrolysis models have been proposed and can be categorized as ones involving only one decomposition reaction, of parallel reactions, of more than one pyrolyzed fraction, and of a continuous distribution of fractions [11].

A number of investigations of biomass pyrolysis kinetics have been reported in the literature. For example, the pyrolysis kinetic of olive stones and almond shells was studied by using the TGA technique [12]. The different kinetic schemes were grouped into two or three overall processes corresponding to the decomposition of hemicellulose, cellulose and lignin. The best results were found for the model describing the biomass decomposition via three independent reactions. Teng et al. [13] studied the kinetics of rice hull pyrolysis by using a combined model of volatile evolutions of four independent parallel reactions. These reactions are associated with the moisture evolution, and the decomposition of hemicellulose, cellulose and lignin. The kinetic study on the pyrolysis of oil-palm solid waste was modeled using the one-step global model and the two-step consecutive reaction model by Guo and Lua [14]. They found that the two-step model could describe well their experimental data. They also suggested that these two reactions are responsible for the softening effect and the formation of an intermediate during the pyrolysis process. Font and co-workers [15] investigated the kinetic pyrolysis of almond shell by using the two-parallel reactions model. This model assumes that the biomass consists of two main fractions having independent pathway of decomposition based on the first-order reaction.

In this study, the internal seed of a longan fruit was used as a biomass resource. This seed has a round shape with an approximate size of 10 mm in diameter. The seed is composed of two main parts, the outer thin black hull and the inner brown kernel. This solid waste is produced from the fruit cannery factories in Thailand and considered to be a potential raw material for activated carbon production [16]. In this work, it was decided to systematically investigate the pyrolysis kinetics of this solid in a thermogravimetric analyzer with an aim to gain basic carbonization conditions necessary for the production of activated carbon during the activation step. The preliminary study of longan seed pyrolysis indicated that the DTG

†To whom correspondence should be addressed.
E-mail: chaiyot@sut.ac.th

diagram exhibited only one major peak. Therefore, it is likely that the decomposition reaction of longan seed may involve only one global reaction. The one-step global model is thus selected to test with the experimental data. However, it is well known that the pyrolysis of lignocellulosic materials is a complex process. Therefore, the two-parallel reactions model is also tried to describe the pyrolysis of longan seed. This model is based on the model proposed by Font et al. [15]. However, in order to increase the model flexibility, it is further assumed in the present study that the reaction order of the first fraction is still first order but that of the second fraction will be optimally searched [17].

THEORY

1. One-step Global Model

The one-step global model is a model containing only one differential rate equation that is based on the best fitted reaction order. It is the simplest kinetic model to describe the decomposition of a pyrolyzed material. The kinetic equation of this model can be represented as

$$\text{Raw material} \xrightarrow{k} \text{Char} + \text{Volatiles} \tag{1}$$

where k is the rate constant which obeys the Arrhenius law. The final form of the rate equation can be written as

$$\frac{d\alpha}{dT} = -\frac{A}{\beta}\exp\left(\frac{-E}{R_g T}\right)(1-\alpha)^n \tag{2}$$

where α is the conversion defined in terms of the reacted mass fraction as

$$\alpha = \frac{w_0 - w}{w_0 - w_f} \tag{3}$$

with w_0, w and w_f being the initial, actual and final mass of the sample, respectively. A is the frequency or pre-exponential factor, E is the activation energy, R_g is the universal gas constant, T is the absolute temperature, n is the order of reaction and β is the constant heating rate. The ordinary differential equation in Eq. (2) was used to fit the experimental data to obtain the parameters A, E and n.

2. Two-parallel Reactions Model

The two-parallel reactions model basically assumes that the reaction is controlled by kinetics regime and the secondary reactions are neglected. This model proposes that the raw material consists of two homogeneous fractions namely M_1 and M_2 and each fraction decomposes simultaneously at different rates at a given temperature, generating the volatile matters and solid char. The scheme of overall reaction is given as

$$\text{Raw material} \xrightarrow{k} \text{Volatile 1} + \text{Volatile 2} + \text{Char} \tag{4}$$

Eq. (4) can be as well represented in the form of two individual parallel reactions as Eq. (5a), and (5b), respectively,

$$M_1 \xrightarrow{k_1} \text{Volatile 1} + \text{Char} \tag{5a}$$

$$M_2 \xrightarrow{k_2} \text{Volatile 2} + \text{Char} \tag{5b}$$

where k_1 and k_2 are the rate constants of each reaction. Now, the residual weight fractions of solid product are defined as follows:

$$\alpha = \frac{m - m_f}{1 - m_f};\quad \alpha_1 = \frac{m_1 - m_{f1}}{1 - m_f};\quad \alpha_2 = \frac{m_2 - m_{f2}}{1 - m_f} \tag{6}$$

where m_f is the final mass fraction of solid char, m_{f1} and m_{f2} are the final mass fractions of the first and second components, respectively. m, m_1 and m_2 are mass fractions of total residual weight, residual weight of component 1 and 2 present at time t, respectively. Obviously,

$$m = m_1 + m_2 \tag{7a}$$

and

$$m_f = m_{f1} + m_{f2} \tag{7b}$$

The rate of decomposition reaction in Eq. (5a) and (5b) can be expressed in terms of α for a constant heating rate, β, based on 1^{st}-order and n^{th}-order regimes for fractions 1 and 2, respectively:

$$\frac{d\alpha_1}{dT} = -\frac{A_1}{\beta}\exp\left(\frac{-E_1}{R_g T}\right)\alpha_1 \tag{8a}$$

$$\frac{d\alpha_2}{dT} = -\frac{A_2}{\beta}\exp\left(\frac{-E_2}{R_g T}\right)\alpha_2^n \tag{8b}$$

Rearranging Eq. (8) and integrating to obtain

$$\int_a^{\alpha_1}\frac{d\alpha_1}{\alpha_1} = -\frac{A_1}{\beta}\int_0^T \exp\left(\frac{-E_1}{R_g T}\right)dT \tag{9a}$$

$$\int_b^{\alpha_2}\frac{d\alpha_2}{\alpha_2^n} = -\frac{A_2}{\beta}\int_0^T \exp\left(\frac{-E_2}{R_g T}\right)dT \tag{9b}$$

where a and b are the initial values of α_1 and α_2, respectively, and they represent the initial weight fractions of the component 1 and component 2 contained in the raw material. They are assumed constant, being the raw material property. Obviously, the relationship between a and b is

$$a + b = 1 \tag{10}$$

The integration of Eq. (9) can be achieved by expressing the exponential term in an asymptotic series and neglecting the higher order terms [17]. The expressions for α_1 and α_2 can be derived as follows:

$$\alpha_1 = \exp\left[\frac{-A_1 R_g T^2}{\beta E_1}\left(1 - \frac{2R_g T}{E_1}\right)\exp\left(\frac{-E_1}{R_g T}\right) + \ln(a)\right] \tag{11a}$$

$$\alpha_2 = \left[\frac{(n-1)A_2 R_g T^2}{\beta E_2}\left(1 - \frac{2R_g T}{E_2}\right)\exp\left(\frac{-E_2}{R_g T}\right) + b^{(1-n)}\right]^{(1/1-n)} \tag{11b}$$

Finally, the total of remaining mass at any temperature is the sum of each residual fraction:

$$\alpha = \alpha_1 + \alpha_2 = \exp\left[\frac{-A_1 R_g T^2}{\beta E_1}\left(1 - \frac{2R_g T}{E_1}\right)\exp\left(\frac{-E_1}{R_g T}\right) + \ln(a)\right] + \left[\frac{(n-1)A_2 R_g T^2}{\beta E_2}\left(1 - \frac{2R_g T}{E_2}\right)\exp\left(\frac{-E_2}{R_g T}\right) + b^{(1-n)}\right]^{(1/1-n)} \tag{12}$$

Eq. (12) was used to test against the experimental data and the six kinetic parameters (a, A_1, E_1, A_2, E_2 and n) are obtained by model fitting.

For the model fitting, the kinetic parameters are optimally searched based on the minimization of sum of square of relative error (S)

defined as

$$S=\sum_{i=1}^{N}\left[\frac{(\alpha_{exp})_i-(\alpha_{cal})_i}{(\alpha_{exp})_i}\right]^2 \quad (13)$$

The subscript i refers to the data point in the total of N data points, α_{exp} represents the experimental value and α_{cal} represents the value calculated from a given set of estimated parameters.

EXPERIMENTAL

The longan seed was collected from the fruit cannery plant of Malee Sampran Public Company Limited in Nakhon Pathom, Thailand. This fresh-longan seed was thoroughly cleaned by water and dried in an oven at 110 °C for 24 h. The pre-dried longan seed was then crushed and sieved to obtain the average particle sizes of 0.05, 0.1, 1.0 and 2.1 mm.

The pyrolysis of longan seed was carried out by using a thermogravimetric analyzer (TGA7 series, Perkin Elmer, USA). The experiment was performed in the non-isothermal pyrolysis mode under the constant flow of nitrogen at the rate of 50 cc/min. The final temperature was fixed at 650 °C, and the heating rates studied were 5, 10, 20, 30, 50 and 100 °C/min.

RESULTS AND DISCUSSION

1. Proximate and Ultimate Analyses of Longan Seed

The proximate and ultimate analyses of longan seed and other biomasses used as raw materials for activated carbon production are listed in Table 1. The fixed carbon content of longan seed is 19.6% with relatively low ash content of 1.7% and the sulfur content is also low at 0.1%. As shown, these values of analyses are comparable with various carbonaceous materials reported in the literature. Therefore, the longan seed used in this study could be used as a potential source for activated carbon preparation.

2. Typical Results of Non-isothermal Pyrolysis of Longan Seed

Results of the non-isothermal pyrolysis of crushed longan seed under nitrogen atmosphere are presented in Fig. 1. Two regions of weight loss behavior upon increasing pyrolysis temperature can be observed. The first region covers the temperature from 100-400 °C. The maximum weight loss rate occurs at 260 °C with the main pyrolysis decomposition of longan seed proceeding through this temperature range. This pyrolysis process involves the evolution of gases and tar from the solid with the formation of residual char. The second region for temperatures above 400 °C corresponds to the aromatization of char structure leading to a relatively small weight change on increasing pyrolysis temperature [19].

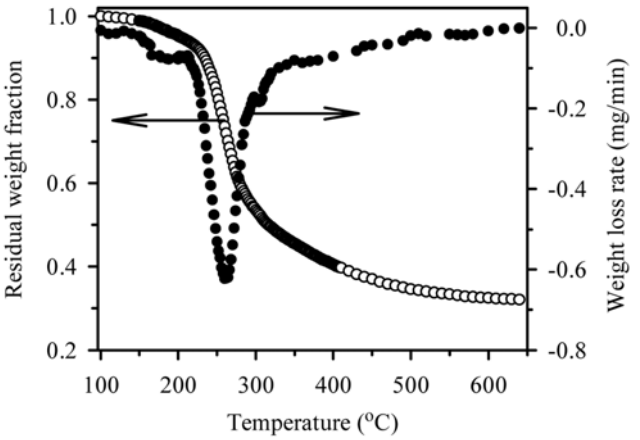

Fig. 1. Typical residual weight fraction (TG) and weight loss rate (DTG) for the non-isothermal pyrolysis of longan seed with particle size 1.0 mm, heating rate 5 °C/min and nitrogen flow rate at 50 cc/min.

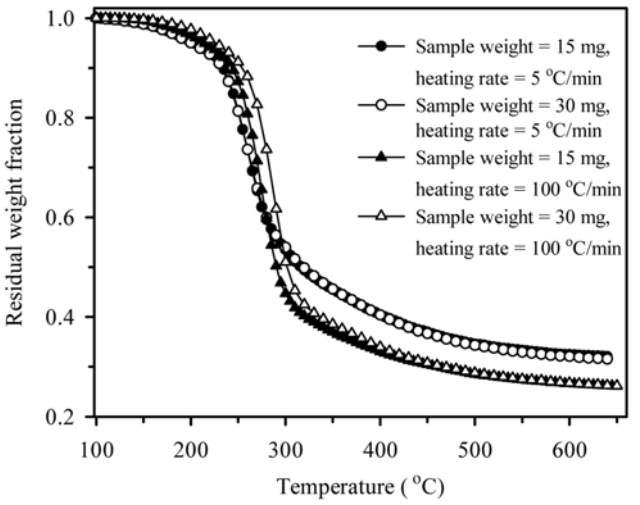

Fig. 2. Effect of initial sample weight on TG curves for the non-isothermal pyrolysis of longan seed at heating rates of 5 and 100 °C/min and particle size of 1.0 mm.

Table 1. Proximate and ultimate analyses of longan seed and some biomasses used for activated carbon preparation

Material	Proximate analysis (dry basis) [wt%]			Ultimate analysis [wt%]				
	Fixed carbon	Volatile matters	Ash	C	H	N	S	O (by diff.)
Longan seed	19.6	78.7	1.7	46.5	6.3	1.4	0.1	45.4
Oil palm shell[a]	19.8	77.6	2.6	NA	NA	NA	NA	NA
Apricot stone[b]	13.7	86.1	0.2	55.6	6.8	0.2	0.1	37.3
Almond shell[b]	11.8	87.2	1.0	51.0	6.3	0.5	0.2	42.0
Cherry stone[b]	10.0	89.4	0.6	53.9	7.1	0.3	0.3	38.4
Grape seed[b]	19.0	78.2	2.8	62.2	7.8	1.6	0.2	28.2

[a]Reference [14]
[b]Reference [18]

3. Initial Sample Weight Effect

Fig. 2 compares the influence of initial sample weight on the TG curves for the weights of 15 and 30 mg at two heating rates of 5 and 100 °C/min. It is seen that there is a measurable influence of the initial weight for the condition of heating rate at 100 °C/min, showing a shift of TG curves to a higher pyrolysis temperature over the range of 240-400 °C as the sample weight is increased. This behavior may arise from the inter-particle transport resistance leading to the heat transfer limitation at a high heating rate condition. It is also interesting to observe that above 400 °C where the main devolatilization has already occurred, the initial sample weight has almost no consequent effect on the solid yield. Thus, it is inferred that the initial sample weight chosen in this study only affects. the increasing of heat transfer resistance under the high heating rate condition. For model analysis of pyrolysis kinetics of longan seed it is implicitly assumed that the process is controlled by the chemical reaction. Therefore, the initial sample weight for 15 mg was chosen for a subsequent series of experiments in this work to eliminate the heat and mass transfer resistances in the pyrolyzed biomass.

4. Particle Size Effect

The TG and DTG results of the longan seed with different particle sizes at the low heating rate of 5 °C/min are shown in Fig. 3. The TG and DTG curves for all particle sizes still show a similar pattern. However, it is found that the final yield depends on the particle size, with larger particle size giving the higher char yield. It is observed that the particle size starts to have an effect at around 270 °C, separating the TG curves into different final yield values. For the DTG data, the temperature range of the main devolatilization appears to start and end at approximately the same temperature for all particle sizes (210-350 °C). However, the magnitude of the maximum rate of weight loss for the smallest particle size (0.05 mm) is evidently higher than those of the other larger sizes.

According to the obtained results, the decrease in particle size resulted in the decrease of char yield. This can be explained by reasoning that a temperature gradient existing in a small particle is less than that in the larger one, indicating lesser heat transfer resistance in the smaller size particle. Under this condition, the pyrolysis should be controlled mainly by the reaction kinetics, thus giving the con-

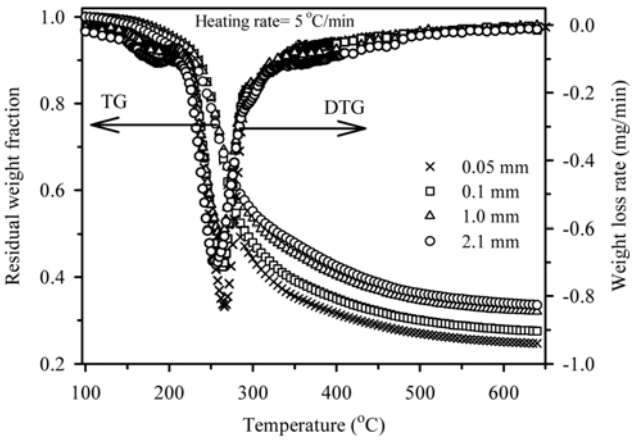

Fig. 3. Effect of particle size on TG and DTG curves for the non-isothermal pyrolysis of longan seed at the heating rate of 5 °C/min.

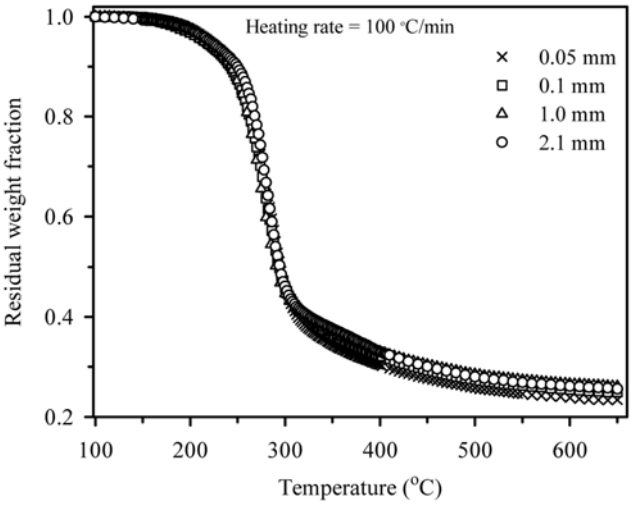

Fig. 4. Effect of particle size on TG curves for the non-isothermal pyrolysis of longan seed at the high heating rate of 100 °C/min.

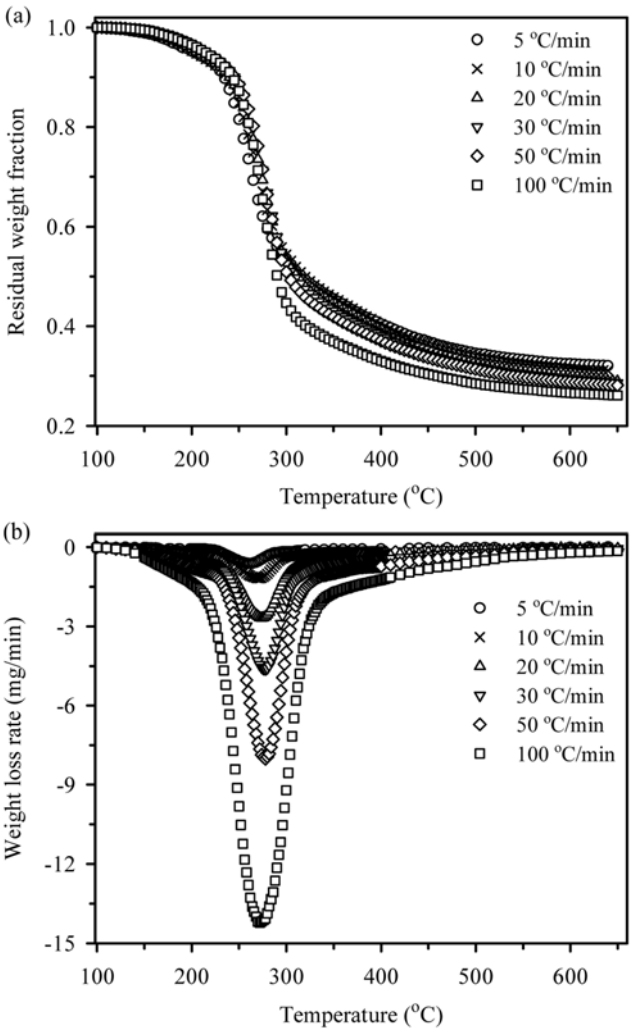

Fig. 5. Effect of heating rate on TG curves (a) and DTG curves (b) for the non-isothermal pyrolysis of longan seed for 1.0 mm particle size.

version of the smaller particle to be higher than that in the larger particle. This observation is also in agreement with the work reported by several previous investigations [14,20].

In addition, the degree of particle size effect on pyrolysis kinetic was found to depend on the heating rate, as shown in Fig. 4 for the TG results obtained at a higher heating rate of 100 °C/min. It is obvious that the difference in solid yields tends to diminish at this high heating rate condition. This is probably attributed to the lowering of particle heat transfer resistance caused by the increasing in the heating rate. This heating rate effect will be further discussed in the following section.

5. Heating Rate Effect

The effect of heating rate on the TG and DTG curves for longan seed with particle size of 1.0 mm is shown in Fig. 5(a) and 5(b),

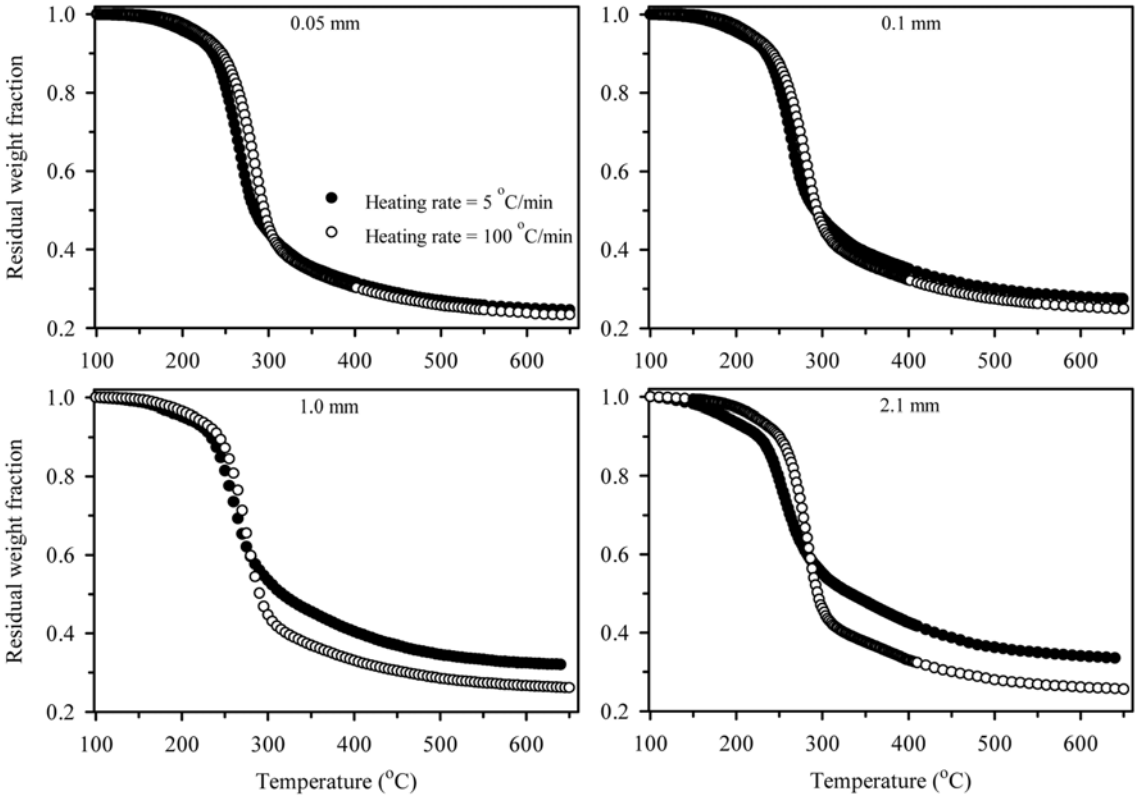

Fig. 6. Comparison of TG curves for the non-isothermal pyrolysis of longan seed at two heating rates of 5 and 100 °C/min for different particle sizes.

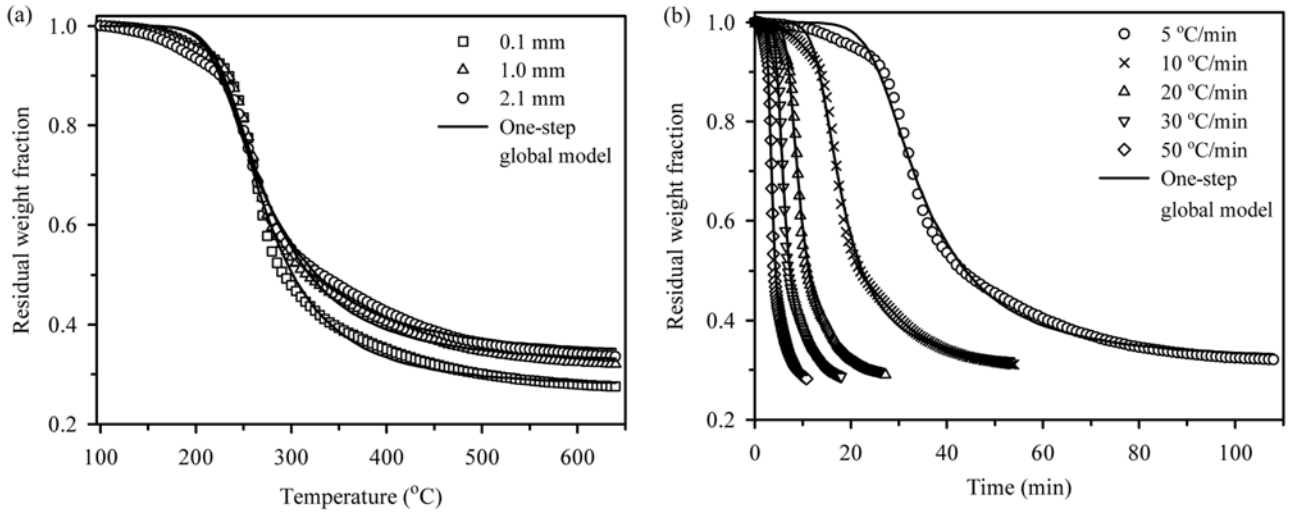

Fig. 7. The effects of particle size (a) and heating rate (b) on the TG curves as compared with the results from the one-step global model fitting.

respectively. There is no significant difference of TG curves in the main devolatilization range of 200-300 °C. However, it is observed that the heating rate significantly affects the maximum weight loss rate of DTG curves, showing the maximum weight loss rate to increase with an increase in the heating rate.

The yield of solid char is also significantly affected by the heating rate in that the yield tends to decrease with increasing in the heating rate. This effect of heating rate on the char yield was also remarked by some previous investigators [14,21]. The solid yield decreases at a high heating rate signifies a decreasing of heat transfer resistance (smaller temperature gradient) due to the marked increase of particle temperature. This heating rate effect should become less for the smaller size particle, because of its lesser heat transfer resistance. This postulation is supported by comparing the heating rate effect at 5 and 100 °C/min for various particle sizes, as displayed in Fig. 6. It is clear that the final yield obtained from heating rates at 5 and 100 °C/min for a particle size of 0.05 mm is approximately the same, while the difference of these two yields in the larger particle size intensifies as the particle size is progressively increased.

6. Model Fitting of Pyrolysis Data

With the appearance of only one peak in the DTG, it might be reasonable that the experimental data could be described by the one-

Table 2. The kinetic parameters obtained from the one-step global reaction model of longan seed pyrolysis

Parameter	Particle size [mm]				Heating rate [°C/min]				
	0.05	0.1	1.0	2.1	5	10	20	30	50
A [min^{-1}]	8.89×10^{9}	1.18×10^{10}	5.16×10^{10}	1.47×10^{11}	5.16×10^{10}	2.34×10^{10}	3.10×10^{10}	1.28×10^{10}	1.64×10^{10}
E [kJ/mol]	122.16	125.48	131.09	133.75	131.09	126.47	125.86	121.16	120.15
n	4.89	4.04	4.64	5.16	4.64	4.51	4.26	4.02	3.84
Max. error [%]	14.49	8.46	5.33	4.64	5.34	5.60	6.73	9.05	10.70

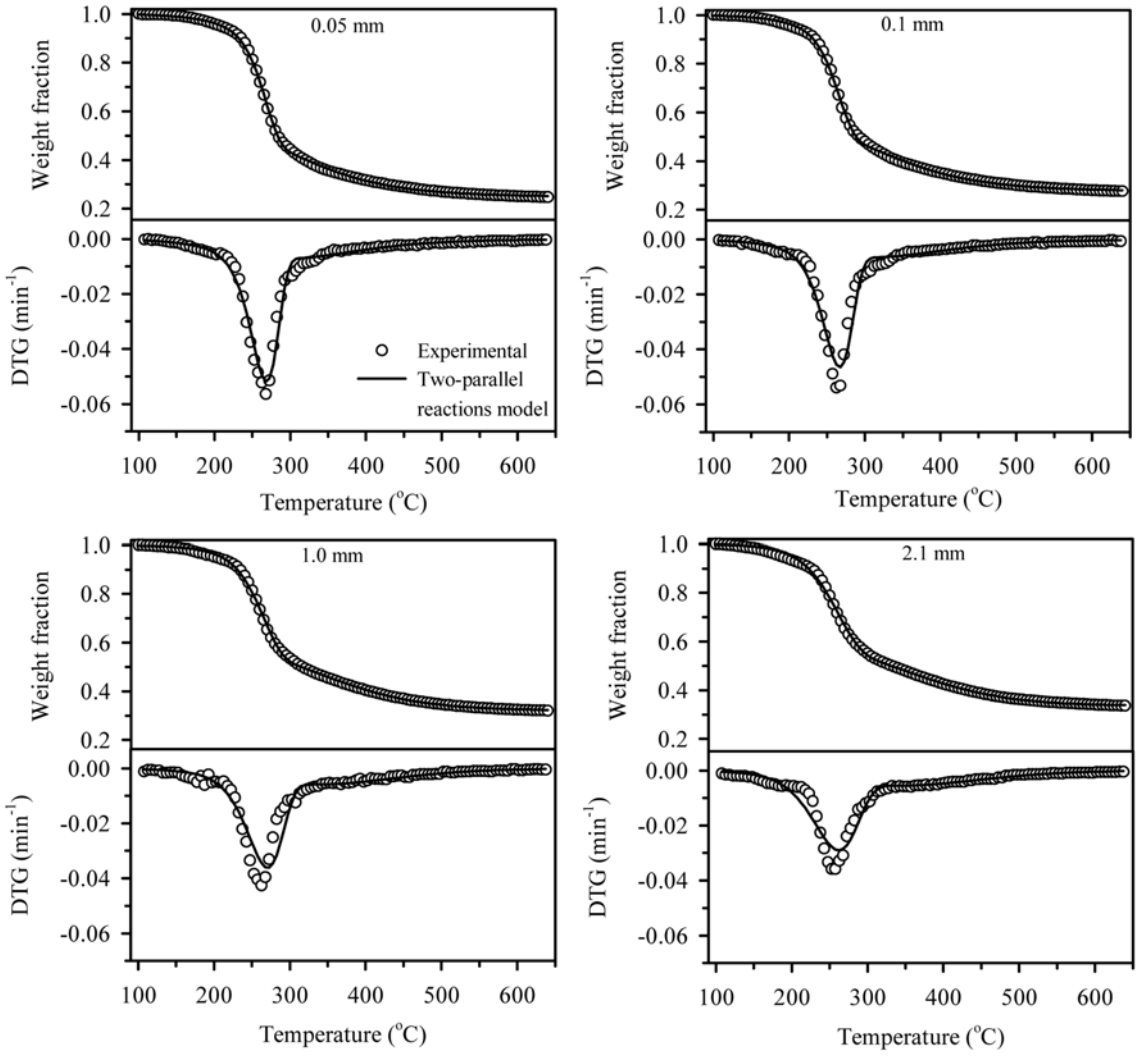

Fig. 8. Comparison of experimental and model computed TG and DTG curves for different particle sizes at a heating rate of 5 °C/min.

step global model. The fitting of the experimental data for different particle sizes and heating rates to the one-step global model is shown in Fig. 7(a) and 7(b), respectively, and the kinetic parameters are listed in Table 2. Overall, it is found that the optimized results from one-step global model agree reasonably with the experimental data. However, the major mismatch is found in the temperature range of 150-220 °C, with the model over-predicting the initial decreasing in mass fraction seen in the experimental data.

Next, the two-parallel reactions model was employed to test against the experimental data. The comparison between the experimental

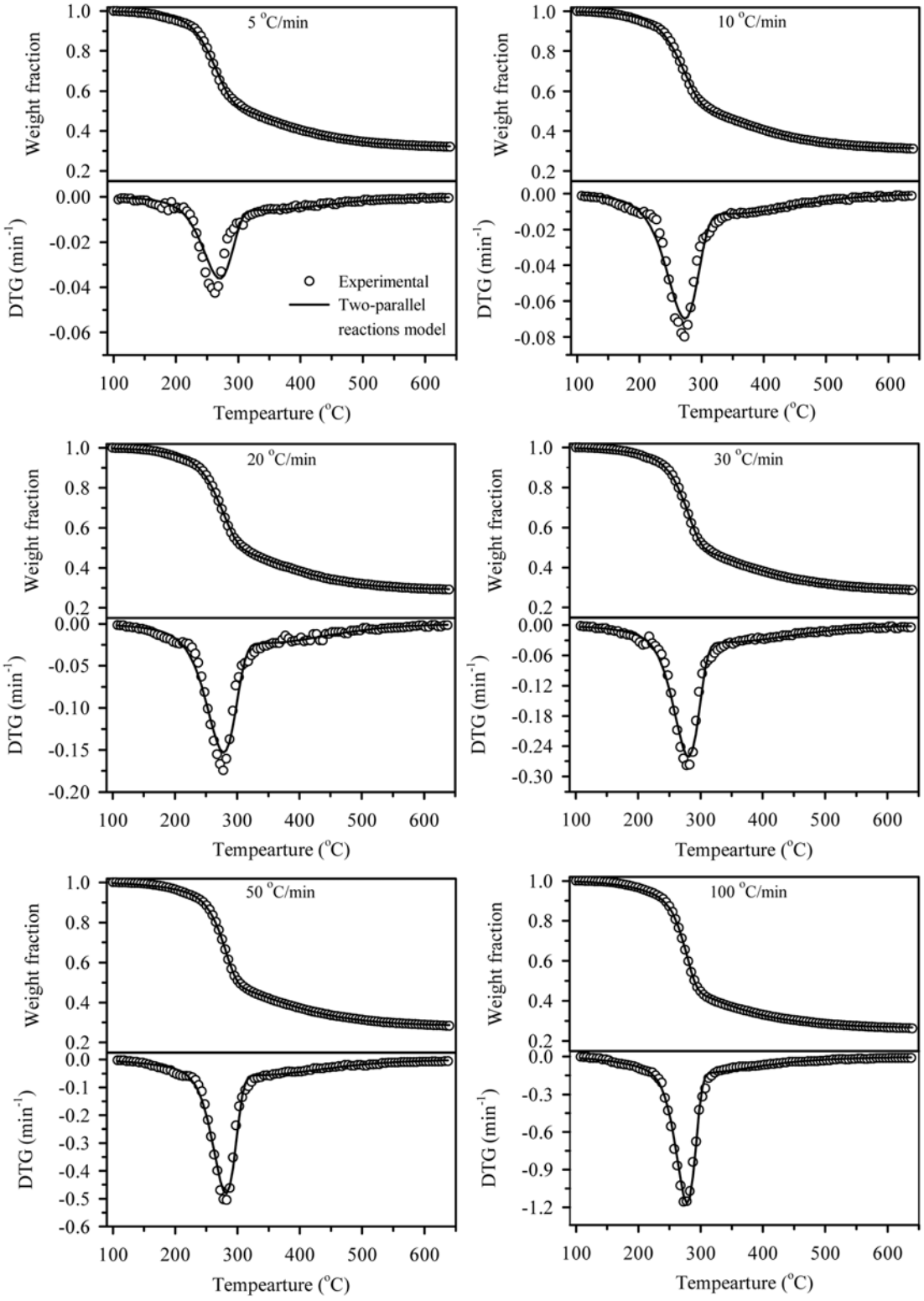

Fig. 9. Comparison of experimental and model computed TG and DTG curves for different heating rates with a particle size of 1.0 mm.

Table 3. The kinetic parameters obtained from the two-parallel reactions model of longan seed pyrolysis

Parameter	Particle size [mm]				Heating rate [°C/min]					
	0.05	0.1	1.0	2.1	5	10	20	30	50	100
a	0.56									
b	0.44									
A_1 [min^{-1}]	4.35×10^{10}	4.65×10^{9}	2.24×10^{7}	1.52×10^{5}	2.23×10^{7}	1.59×10^{7}	2.04×10^{8}	1.78×10^{10}	8.62×10^{11}	4.60×10^{14}
E_1 [kJ/mol]	134.43	124.31	100.96	79.00	100.96	97.93	107.04	125.62	140.81	164.87
A_2 [min^{-1}]	2.92	1.52	0.56	0.30	0.56	0.63	1.07	1.54	2.27	31.46
E_2 [kJ/mol]	35.12	33.47	31.26	29.42	31.26	29.41	28.52	28.14	27.08	32.30
n	1.66	1.55	1.31	1.18	1.31	1.22	1.19	1.22	1.23	1.62
Max. error [%]	2.89	3.08	2.32	2.26	2.32	1.72	1.96	2.05	1.63	2.14

data and the model prediction for the effects of particle size and heating rate is shown in Fig. 8 and Fig. 9, respectively, while the kinetic parameters are listed in Table 3. Overall, the two-parallel reactions model can describe the experimental data extremely well for all particle sizes and heating rates studied, with the maximum deviation being in the range of 1.63-3.08%. The two-parallel reactions model can account for the mismatch previously predicted by the one-step global model in the temperature range of 150-220 °C. Therefore, the assumption of the two parallel decomposition scheme proposed in this work appears to be satisfactorily sound. The model fitting

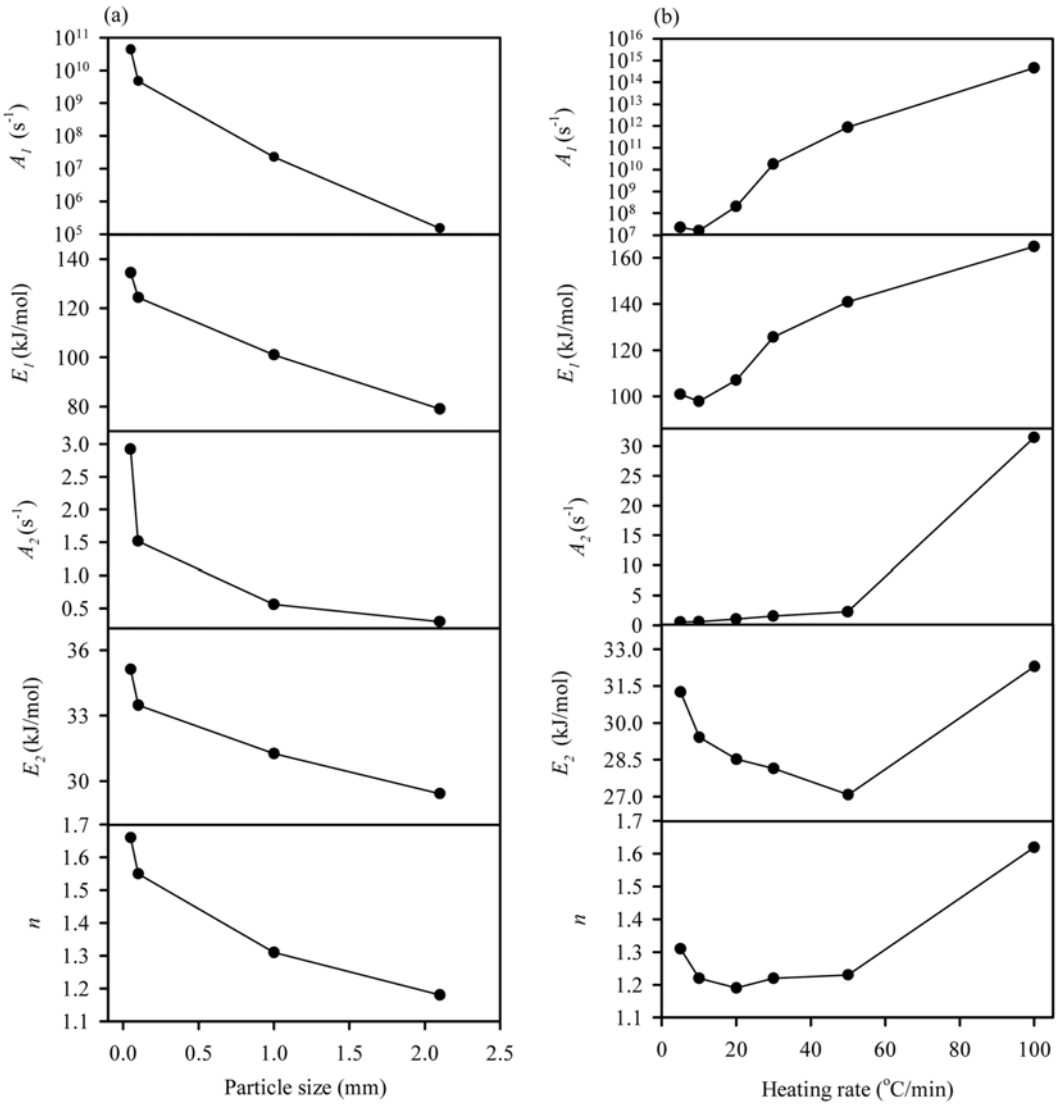

Fig. 10. The dependence of fitted kinetic parameters from the two-parallel reactions model on particle size (a) and heating rate (b).

gave the values of the fraction parameters a and b as 0.56 and 0.44, respectively.

The effects of heating rate and particle size on the kinetic parameters are shown in Fig. 10(a) and 10(b) for clearer observation. Fig. 10(a) shows a continued decreasing of all parameter values as the particle size is increased. The order of reaction 2 (n) decreases from 1.66 to 1.18 as the particle size is increased from 0.05 to 2.1 mm. On the other hand, the kinetic parameters as affected by the variation in the heating rate do not display a definite trend, as seen in Fig. 10(b). It should be noted that the model reaction is based on the assumption of pure kinetic control, neglecting the effect of heat and mass transfer resistances. Under this assumption, the kinetic parameters should be independent of particle size and heating rate. However, the variation of kinetic parameters discovered here could be ascribed to the complex scheme of pyrolysis reaction and also the influence of some heat and mass transfer resistance still existing in the real process.

All results from the model fitting show that the pre-exponential factor and activation energy in the first fraction are higher than that

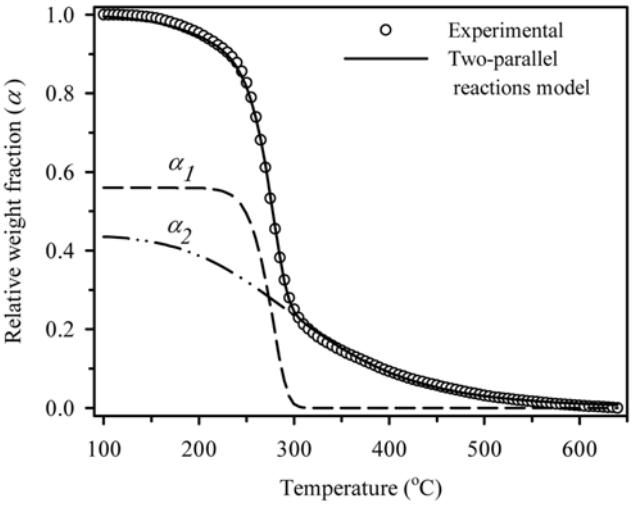

Fig. 11. The relative weight fraction (α) derived from the reaction schemes for a particle size of 1.0 mm at heating rate of 100 ^{o}C/min.

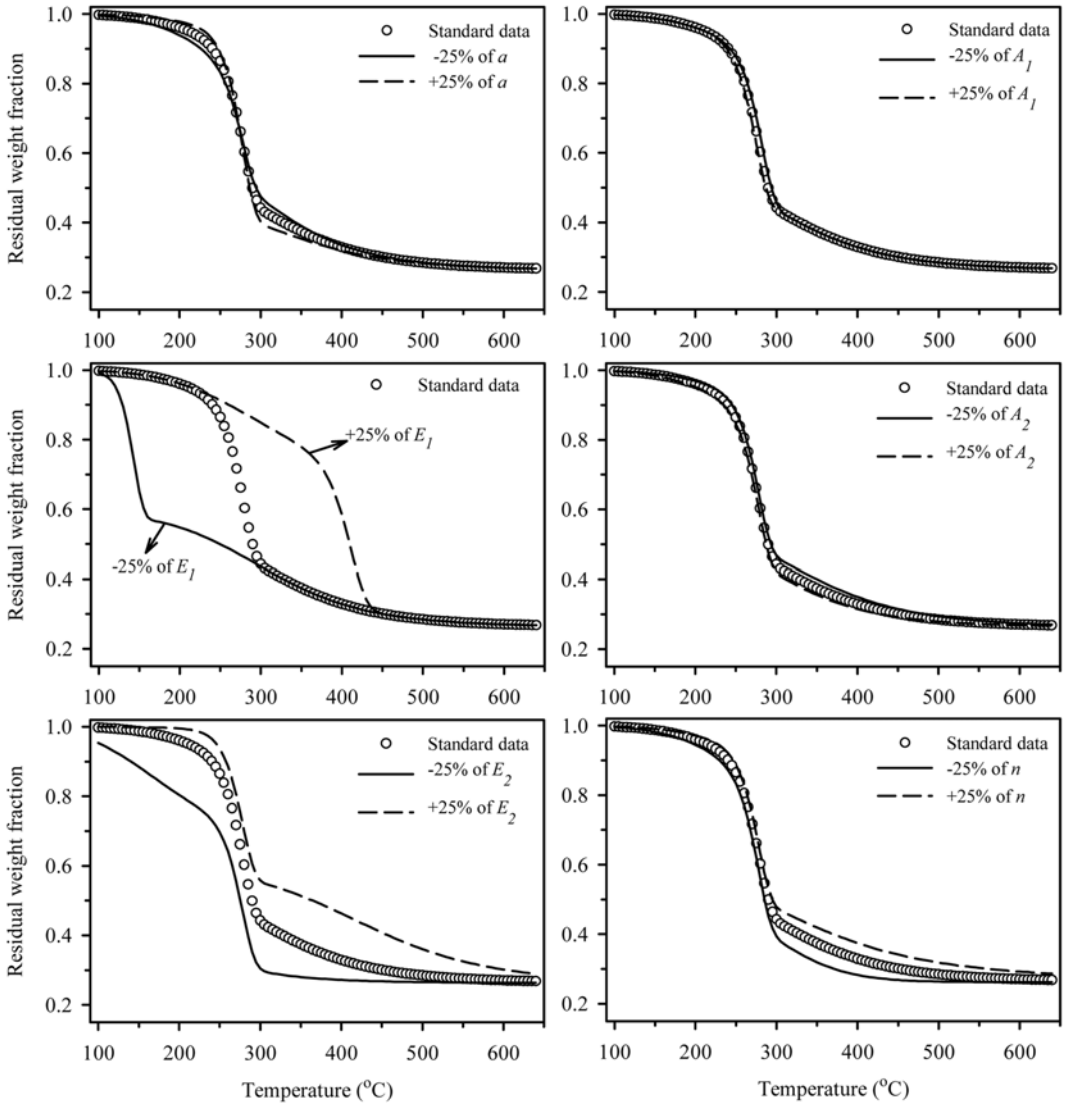

Fig. 12. The sensitivity analysis of kinetic parameters on the weight fraction remaining.

in the second fraction. These A_1 and E_1 parameters values are 1.52×10^5-4.60×10^{14} min^{-1} and 79.00-164.87 kJ/mol and A_2 and E_2 are 0.30-31.46 min^{-1} and 27.08-35.12 kJ/mol, respectively. It is clearly seen that the parameters of reaction 2 (A_2 and E_2) are much lower than those of reaction 1 (A_1 and E_1). This behavior could be further examined from the contribution of each pyrolysis reaction as shown in Fig. 11. α_1 and α_2 are referred to as the decomposition of the biomass composition in fraction a and b, respectively. The results indicate that fraction α_1 sharply decreases at 220 °C and reaches a final fractional value at 300 °C. However, α_2 decreases continuously from the initial temperature of 100 °C up to the final temperature. These decomposition behaviors suggest that reaction 1 proceeds faster than reaction 2, as reflected by a much higher value of A. Tsamba et al. [22] summarized the kinetic parameters values of biomass components from the literatures and their studies as follows: E_{min}(hemicellulose)=147.24±38.52 kJ/mol, E_{max}(hemicellulose)=172.75±39.44 kJ/mol, E_{min}(cellulose)=176.92±42.41 kJ/mol and E_{max}(cellulose)=248.64±25.75 kJ/mol. By comparing with these reported results, it was suggested that the values of activation energy obtained for reaction 1 derived from the present study (79.00-164.87 kJ/mol) could be attributed to the thermal decomposition of hemicellulose. Reaction 2 should correspond to the decomposition of lignin since the activation energy obtained in this work (27.08-35.12 kJ/mol) is in the range of 34-65 kJ/mol for lignin decomposition as reported by Varhegyi and co-workers [23].

7. Sensitivity Analysis of the Two-parallel Reactions Model

The two-parallel reactions model contains six kinetic parameters, thus making it difficult to assess the accuracy of the model with respect to the variation of model parameters. Therefore, the analysis of the sensitivity of each parameter on the model results was performed by changing its value by ±25% while keeping the remaining parameters constant. The analysis was performed using the data of the 1.0 mm longan seed particle at the heating rate of 100 °C/min. The resulting change in TG curves is compared to the standard data computed from the optimized parameters, and is displayed in Fig. 12. The maximum deviation derived from this sensitivity analysis is listed in Table 4.

It is observed that the +25% of a (increasing fractional composition for reaction 1) gives a weight fraction higher than the standard data in the temperature range of 200-275 °C but lower in the temperature range of 275-400 °C, while for the −25% change the decomposition behaviors show the opposite direction. The change of pre-exponential factors, A_1 and A_2, describes how fast the decomposition rate proceeds: the higher the A values the faster is the rate of reaction. An increasing in A_1 is observed to decrease the weight fraction in the temperature range of 250-300 °C. The increasing of A_2 also causes a decreasing of weight fraction through the entire range of temperature for reaction 2. However, it appears that the TGA data are least sensitive to changes in both A_1 and A_2, as can be observed from Table 4. The largest sensitivity is found for the activation energies of both reactions (E_1 and E_2) (see %max. deviation in Table 4) and this parametric effect is more pronounced for reaction 1. The activation energy corresponds to the energy barrier of the reaction with the higher value indicating the slower of the reaction rate. Therefore, the increasing in the activation energy should prolong the decomposition reaction to the higher temperature or longer time. The behaviors seen in the sensitivity analysis support this result; for example, as shown in Fig. 12, the main devolatilization of reaction 1 is prolonged to the temperature range 350-450 °C with +25% of E_1, and the +25% of E_2 also delays the reaction 2 to decompose at the higher temperature. The increasing of reaction order n also delays the biomass decomposition, yielding the higher residual weight fraction than the lesser order reaction does.

Table 4. Sensitivity analysis reported as percent maximum deviation of pyrolysis model parameters from the optimized parameters for the pyrolysis of longan seed with 1.0 mm particle size and 100 °C/min heating rate

Sensitivity analysis	Max. deviation [%]					
	a	A_1	E_1	A_2	E_2	n
+25%	9.72	4.85	110.68	5.56	40.19	13.32
−25%	8.29	8.12	43.96	8.60	31.90	14.85

CONCLUSIONS

The non-isothermal pyrolysis of longan seed exhibited a TG curve with sigmoid shape and showed only one major peak in the DTG curve. The condition of the particle size 1.0 mm and at the heating rate of 5 °C with the final temperature being at 650 °C produced the char yield of 30% and the main devolatilization occurred in the temperature range of 210-330 °C. The heat transfer resistance was increased by both increasing in particle size and decreasing in heating rate, resulting in a corresponding increase of char yield. The kinetics of the decomposition of longan seed could be extremely well described by the two-parallel reactions model. The initial fraction of the biomass components derived from this model was 0.56 and 0.44 for reaction 1 and reaction 2, respectively. The pre-exponential factors in the range 1.52×10^5-4.60×10^{14} min^{-1} and activation energy ranging from 79.00-164.87 kJ/mol were obtained for reaction 1, the range of which depending on the particle size and the applied heating rates. Reaction 2 was well fitted with the reaction order of 1.18-1.62, the pre-exponential factors of 0.30-31.46 min^{-1} and activation energy of 27.08-35.12 kJ/mol. These values of activation energy suggested that reaction 1 and 2 could be represented by the decomposition of hemicellulose and lignin, respectively. The sensitivity analysis on the predicted TG curve for a particle size 1.0 mm at the heating rate 100 °C/min showed the highest sensitivity towards the changes in the activation energies of both reaction 1 and 2.

ACKNOWLEDGMENT

Financial supports from the Thailand Research Fund (TRF) through the Royal Golden Jubilee Ph.D. Program (Grant No. PHD/0087/2543) is gratefully acknowledged.

REFERENCES

1. S-S. Kim, F. A. Agblevor and J. Lim, *J. Ind. Eng. Chem.*, **15**, 247 (2009).
2. H. J. Park, Y.-K. Park, J.-I. Dong, J.-S. Kim, J.-K. Jeon, S.-S. Kim, J. Kim, B. Song, J. Park and K.-J. Lee, *Fuel Process. Technol.*, **90**, 186 (2009).

3. H. J. Park, J.-I. Dong, J.-K. Jeon, Y.-K. Park, K.-S. Yoo, S.-S. Kim, J. Kim and S. Kim, *Chem. Eng. J.*, **143**, 124 (2008).
4. Y.-H. Park, J. Kim, S.-S. Kim and Y.-K. Park, *Bioresour. Technol.*, **100**, 400 (2009).
5. H. J. Park, J.-I. Dong, J.-K. Jeon, K.-S. Yoo, J.-H. Yim, J. M. Sohn and Y.-K. Park, *J. Ind. Eng. Chem.*, **13**, 182 (2007).
6. H. I. Lee, H. J. Park, Y.-K. Park, J. Y. Hur, J.-K. Jeon and J. M. Kim, *Catal. Today*, **132**, 68 (2008).
7. H. J. Park, J.-K. Jeon, J. M. Kim, H. I. Lee, J.-H. Yim, J. Park and Y.-K. Park, *J. Nanosci. Nanotechnol.*, **8**, 5439 (2008).
8. H. B. Goyal, D. Seal and R. C. Saxena, *Renewable Sustainable Energy Rev.*, **12**, 504 (2008).
9. S. Kim and Y. Eom, *Korean J. Chem. Eng.*, **23**, 409 (2006).
10. R. R. Baker, *Thermochim. Acta*, **23**, 201 (1978).
11. J. A. Conesa, A. Marcilla, J. A. Caballero and R. Font, *J. Anal. Appl. Pyrol.*, **58-59**, 617 (2001).
12. J. A. Caballero, J. A. Conesa, R. Font and A. Marcilla, *J. Anal. Appl. Pyrol.*, **42**, 159 (1997).
13. H. Teng, H.-C. Lin and J.-A. Ho, *Ind. Eng. Chem. Res.*, **36**, 3947 (1997).
14. J. Guo and A. C. Lua, *Biomass Bioenergy*, **20**, 223 (2001).
15. R. Font, A. Marcilla, E. Verdu and J. Devesa, *J. Anal. Appl. Pyrol.*, **21**, 249 (1991).
16. S. Junpirom, D. D. Do, C. Tangsathitkulchai and M. Tangsathitkulchai, *Carbon*, **43**, 1936 (2005).
17. P. Luangkiattikhun, C. Tangsathitkulchai and M. Tangsathitkulchai, *Bioresour. Technol.*, **99**, 986 (2006).
18. K. Gergova, N. Petrov and S. Eser, *Carbon*, **32**, 693 (1994).
19. T. Fisher, M. Hajaligol, B. Waymack and D. Kellogg, *J. Anal. Appl. Pyrol.*, **62**, 331 (2002).
20. H. Haykiri-Acma, *J. Anal. Appl. Pyrol.*, **75**, 211 (2006).
21. J. F. Gonzalez, J. M. Encinar, J. L. Canito, E. Sabio and M. Chacon, *J. Anal. Appl. Pyrol.*, **67**, 165 (2003).
22. A. J. Tsamba, W. Yang and W. Blasia, *Fuel Process. Technol.*, **87**, 523 (2006).
23. G. Varhegyi, M. J. Antal, E. Jakab and P. Szabo, *J. Anal. Appl. Pyrol.*, **42**, 73 (1997).